

**NPL REPORT AS 59**

**EURAMET 1002:  
International comparability in measurements of trace water vapour**

**P J Brewer, M J T Milton, P M Harris, S A Bell, M Stevens, G Scace,  
H Abe and P Mackrodt**

**JUNE 2011**



**Draft Report on EURAMET 1002**  
**International comparability in measurements of trace water vapour**

P J Brewer, M J T Milton, P M Harris (NPL, Acoustics & Ionising  
Radiation Division), S A Bell (NPL, Engineering Measurement Division),  
M Stevens (NPL, Engineering Measurement Division),  
G Scace (NIST,USA), H Abe (NMIJ, Japan), P Mackrodt (PTB,  
Germany)

Analytical Science Division, Operation Directorate

© Queen's Printer and Controller of HMSO, 2011

ISSN 1754-2928

National Physical Laboratory  
Hampton Road, Teddington, Middlesex, TW11 0LW

Extracts from this report may be reproduced provided the source is acknowledged  
and the extract is not taken out of context.

Approved on behalf of NPLML by Alan Brewin, Division Head.

## CONTENTS

<b>1</b>	<b>INTRODUCTION</b> .....	<b>1</b>
<b>2</b>	<b>PARTICIPANTS</b> .....	<b>2</b>
<b>3</b>	<b>COMPARISON PROTOCOL</b> .....	<b>2</b>
	3.1    NATIONAL INSTITUTE OF STANDARDS AND TECHNOLOGY (NIST) METHOD	4
	3.2    NATIONAL PHYSICAL LABORATORY GAS METROLOGY AND TRACE ANALYSIS GROUP (NPL-GMTA) METHOD .....	5
	3.3    NATIONAL PHYSICAL LABORATORY, TEMPERATURE AND HUMIDITY GROUP (NPL-TH) METHOD .....	6
	3.4    PHYSIKALISCH-TECHNISCHE BUNDESANSTALT (PTB) METHOD .....	7
	3.5    NATIONAL METROLOGY INSTITUTE OF JAPAN (NMIJ) METHOD.....	8
<b>4</b>	<b>RESULTS</b> .....	<b>9</b>
	4.1    CALCULATION OF REFERENCE VALUES .....	11
<b>5</b>	<b>CONCLUSION</b> .....	<b>14</b>
<b>6</b>	<b>REFERENCES</b> .....	<b>15</b>
<b>7</b>	<b>APPENDIX – DATA FROM PARTICIPANTS</b> .....	<b>16</b>
<b>8</b>	<b>ANNEX</b> .....	<b>22</b>



## 1 INTRODUCTION

The measurement of trace amounts of water in purge and process gases is of critical importance for a number of manufacturing processes, perhaps none more so than the fabrication of semiconductor devices. The semiconductor industry recognises water as one of the most difficult impurities to remove from gas distribution systems. The industry trend is moving towards larger wafer diameters, which in turn will lead to lower process pressures and gas flows. There is clear evidence that the presence of contamination in semiconductor gases has a measurable impact on the quality and performance of semiconductor devices. Large-scale integration devices, with the smallest features in the 3  $\mu\text{m}$  range, may not be affected adversely by trace impurities. However, yields of very large scale integration and ultra large-scale integration devices, in which line-widths are smaller than 2  $\mu\text{m}$ , are very sensitive to trace impurities. In these conditions the moisture and gases adsorbed on the inner surfaces of processing equipment are readily desorbed into the gas flow affecting processing significantly. Consequently, semiconductor manufacturers are constantly reducing target levels of water present in purge and process gases.

Suppliers of ultra-high-purity gases for the semiconductor industry are required to certify the quality of their products, as are the suppliers of gas purification equipment, which is almost always used immediately upstream of any tooling to ensure the highest purity at point-of-use. As the purity of gases improves, suppliers and users are faced with the problem of quantifying contamination and ensuring that the gases are within specifications at point of use.

There are several established methods for determining trace water vapour found in inert gases. Instruments based on the chilled mirror principle which measures the dew-point of the gas are commonplace, as are those based on the quartz crystal adsorption principle which measures the adsorption of water vapour into a crystal with a hygroscopic coating. Most recently, spectroscopic instruments such as those employing cavity ringdown spectroscopy (CRDS) have become available. As these techniques are refined, so the claimed response times and detection limits are pushed even lower. The development of analytical techniques capable of measuring ever-decreasing impurity levels must be coupled with traceable calibration.

The calibration of such instruments below the 1  $\mu\text{mol/mol}$  level has until recently been a difficult task with few facilities available to generate reliable water standards at these levels. A small number of NMIs (national metrology institutes) are now in the position to offer such calibrations using standards based on dynamic generation techniques. Whilst some of these facilities have been in use for a number of years, little work has been done to compare the facilities and quantify the variability between the standards and their accuracy at amount fractions that are of interest to industrial users of trace water analysers. This European Association of National Metrology Institutes (EURAMET) comparison addresses this issue by comparing a number of trace water vapour generation facilities at several NMIs.

## 2 PARTICIPANTS

**Table 1 EURAMET project 1002 participants**

Abbreviation	Participant	Country	Analyst
NIST	National Institute of Standards and Technology	US	Greg Scace
NPL-GMTA	National Physical Laboratory Gas Metrology and Trace Analysis Group	UK	Paul Brewer
NPL-TH	National Physical Laboratory Temperature and Humidity Group	UK	Mark Stevens
PTB	Physikalisch-Technische Bundesanstalt	DE	Peter Mackrodt
NMIJ	National Metrology Institute of Japan	JP	Hisashi Abe

## 3 COMPARISON PROTOCOL

A Tiger Optics Laser Trace 6000 CRDS (travelling standard 1) and a Tiger Optics Halo CRDS (travelling standard 2) were sent to each participating laboratory. Participants used these instruments to measure their dynamic standard over the range 10 – 2000 nmol/mol.

CRDS operates by tuning a laser source to the unique molecular fingerprint of the target compound. By measuring the time it takes the light to "ring-down", an accurate molecular count is received in milliseconds. A continuous wave diode laser emits a directed beam of light energy through an ultra-high reflective mirror into the absorption cell (cavity). The light reflects back and forward between two ultra-high reflective mirrors multiple times. When the photodiode detects a preset level of light energy, the light source is shuttered or diverted from the cavity. On each successive pass, a small amount of light or ring-down signal emits through the second mirror and is sensed by the light detector. Once the light "rings down", the detector achieves a point of zero light energy in milliseconds, and the measurement is complete. A computer-controlled system tunes the laser off the absorption peak for water to determine the tau zero ( $\tau_{ZERO}$ ) value, equivalent to a zero baseline correction. It tunes back to the absorption peak to determine the tau measure ( $\tau$ ) value, dependent on the amount fraction of water. The amount fraction of water is calculated using equations 1-3 below.

$$\tau_{ZERO} = \frac{d}{c(1-R)} \quad (1)$$

$$\tau(\nu) = \frac{d}{c(1-R + \sigma(\nu)Nd)} \quad (2)$$

$$N = \frac{1}{c\sigma(\nu)} \left( \frac{1}{\tau(\nu)} - \frac{1}{\tau_{ZERO}} \right) \quad (3)$$

where  $c$  is the speed of light,  $d$  is the cell length,  $R$  is the mirror reflectivity,  $N$  is the amount fraction of water,  $\sigma$  is the absorption cross section,  $\tau$  is the ring down time and  $\nu$  is the frequency.

All measurements were made in a matrix of nitrogen, except those of NPL-TH which were made in air. Measurements were made in ascending order from the lowest amount fraction. Measurements were then made in descending order from the highest to the lowest amount fraction. The sequence was repeated twice such that three measurements were made at 10 nmol/mol. At the two instances in the experiment where a mixture of 2000 nmol/mol was generated, an additional measurement was made (making a total of four). This was achieved by deviating the generated water vapour standard to an



amount fraction higher than 2000 nmol/mol after the first measurement, before resetting to 2000 mol/mol for an additional measurement. The sequence of measurements is shown in figure 1.

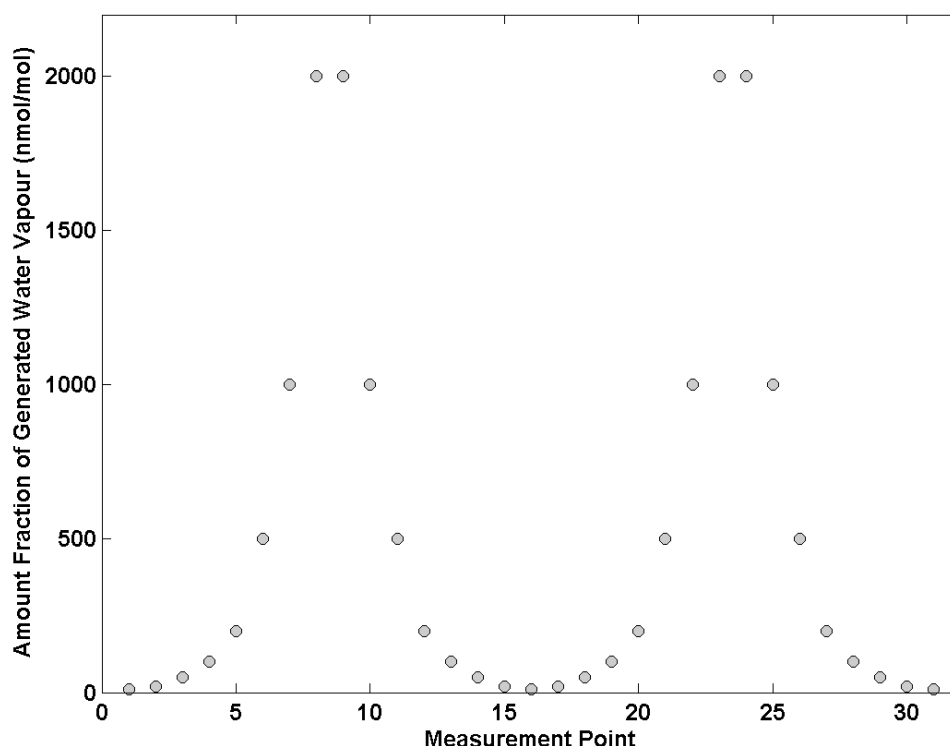


**Figure 1** Sequence of measurements in the comparison protocol.

Tiger Optics commissioned all analyser hardware and software prior to release of the transfer standards for the comparison. No changes to hardware or software were made by the participating laboratories, besides those specified by the supplier for normal operation and diagnostic purposes. All measurement data relating to the comparison was deleted from the travelling standard prior to shipping to the next participant. On receipt of the analysers, inlet lines were purged, providing adequate gas flow. Undue exposure to ambient atmosphere was avoided. The laser current, laser temp, threshold, tau measure, tau zero and wavelength were noted. An “auto-tune” was run and any change in tau zero on the front panel was noted. The peak position was optimised by the instrument’s software and any changes in laser current and laser temperature readings were noted (travelling standard 1 only). When the concentration reading began to approach the expected value, another tune was run (just tau zero). After the tune was complete any changes in readings were noted. The process normalises the analyser. Table 2 displays the timescale of the measurements.

**Table 2** Timescale of measurements

Abbreviation	Participant	Country	Measurement Period
NIST	National Institute of Standards and Technology	US	Oct – Nov 2007
NPL-GMTA	National Physical Laboratory Gas Metrology and Trace Analysis Group	UK	Mar 2008
NPL-TH	National Physical Laboratory Temperature and Humidity Group	UK	Apr 2008
PTB	Physikalisch-Technische Bundesanstalt	DE	Sep-Dec 2008
NMIJ	National Metrology Institute of Japan	JP	Apr 2009
NIST	National Institute of Standards and Technology	US	Apr-Oct 2010

## 3.1 NATIONAL INSTITUTE OF STANDARDS AND TECHNOLOGY (NIST) METHOD

A schematic of the Low Frost Point Generator (LFPG) used at NIST is shown in figure 2.

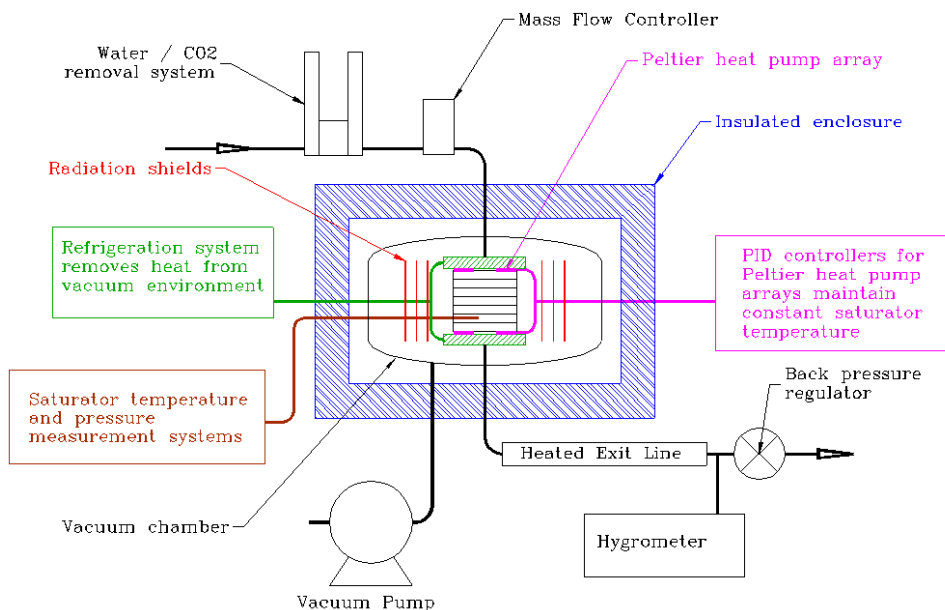


**Figure 2 Schematic of the NIST Low Frost Point Generator (LFPG).**

The LFPG saturates an inert gas stream with water vapour by flowing the gas over a plane surface of isothermal ice at known temperature and pressure. By ensuring that the inlet gas stream has reached thermodynamic equilibrium with the generator saturator, the mole fraction of water vapour in the gas phase,  $x_w$ , can be calculated from first principles, and is proportional to the vapour pressure of the ice,  $e_w(T)$  and the so-called water vapour enhancement factor,  $f(T,P)$ . This factor is close to unity and accounts for departures from ideal solution behaviour as well as non-ideal gas effects [1,2]. Assuming that the saturator ice and sample stream are in local thermodynamic equilibrium, then, at a total pressure,  $P_s$ , and system absolute temperature,  $T_s$ , the amount fraction of water vapour is:

$$x_w = \frac{e_w(T_s)}{P_s} f(T_s, P_s) \quad (4)$$

in which the subscript s indicates conditions in the saturator. Equation 4 represents the central theoretical basis for the use of the LFPG as a humidity standard. The predicted values of LFPG-produced water vapour mole fractions are based on the ice vapour pressure correlation of Wexler [1] and the enhancement factor equation for water vapour/air mixtures [2], both of which are referenced to the International Temperature Scale of 1968, IPTS-68. To use these equations, the measured temperatures (which are referenced to the International Temperature Scale of 1990, ITS-90) are first converted to IPTS-68 [3].

Measurements of the gas frost-point temperature made downstream of the saturator (as for example with a chilled mirror hygrometer) must be related to the saturator conditions. Assuming that the water vapour mole fraction is conserved, and assuming that the hygrometer and sample stream are in local thermodynamic equilibrium, then

$$x_w = \frac{e_w(T_s)}{P_s} f(T_s, P_s) = \frac{e_w(T_h)}{P_h} f(T_h, P_h) \quad (5)$$

in which the subscript h indicates conditions in the hygrometer.

### 3.2 NATIONAL PHYSICAL LABORATORY GAS METROLOGY AND TRACE ANALYSIS GROUP (NPL-GMTA) METHOD

The NPL trace water vapour facility has a capability for generating an adjustable level of trace water (between 2 – 2000 nmol/mol) by using continuous accurate measurements of mass loss from a permeation device coupled with a dilution system based on an array of critical flow orifices.[4] A schematic of the facility is shown in figure 3.

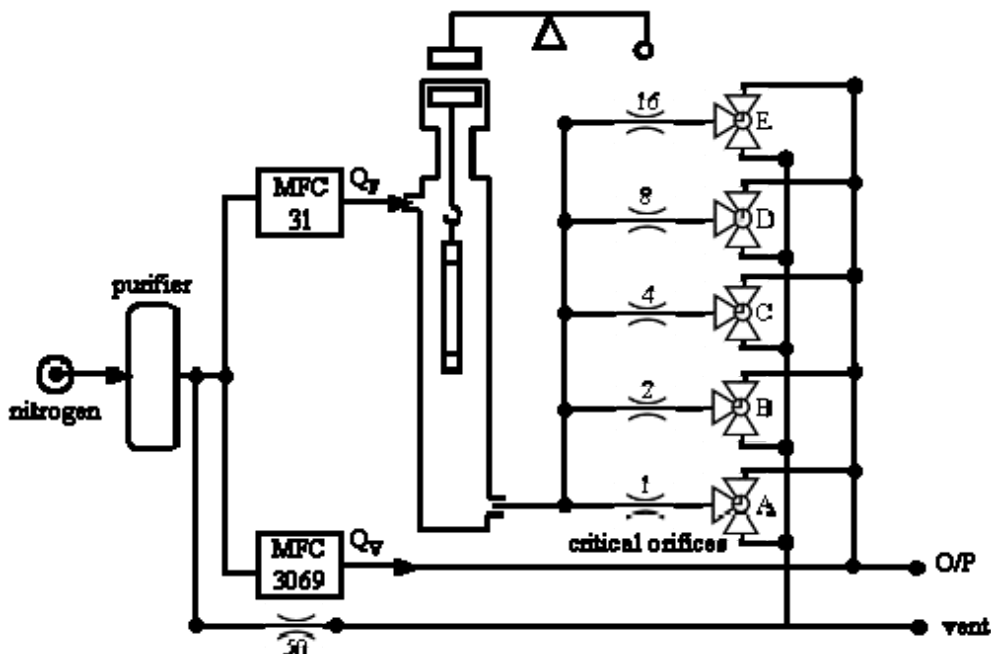


**Figure 3 Schematic of the NPL trace water vapour facility. Valves A to E are switched to flow gas from the permeation source to either the output (O/P) or to the vent. This maintains a constant pressure in the permeation chamber. The output (O/P) is connected to the gas analyser.**

The diluent gas is supplied from ultra high purity nitrogen cylinders (Air Products, BIP), which passes through a purifier system (SAES Getter Monotorr). The output from the purifier passes directly to two mass flow controllers (MFCs) that control  $Q_V$  and  $Q_F$  at nominal flows of 5 and 0.05 standard litres per minute respectively. Flow  $Q_F$  passes over a water vapour permeation source that is magnetically suspended from a microbalance (Rubotherm) with on-line weighing accurate to 1  $\mu\text{g}$ . The use of a magnetically coupled balance enables an in-line continuous weighing measurement to be made and minimises the wetted surface area of the system, reducing the time taken to achieve a stable standard on start-up and when changing flow or temperature. The permeation source is temperature stabilised to  $\pm 0.05\text{ }^\circ\text{C}$  to ensure a stable permeation rate and negligible balance drift. The main components of the facility are sealed in a temperature stabilised enclosure, which is continuously purged with dry nitrogen. All surfaces contacted by the gas are metal (pipework is electropolished seamless stainless steel tubing with clean room welded face seal fittings). A key feature of the design is that the fraction of water vapour is constant throughout the system up to the final blending stage: hence the area exposed to changeable fractions of water vapour is minimised.

The flow from the permeation source ( $Q_T$ ) is split by an array of critical orifices (LN industries SA). The flows through the critical orifices are weighted in binary ratios since this provides an efficient means of adjustment whilst retaining constant resolution when setting the flow. Since it is the ratio of the flows through the critical orifices that determines the dilution, it is not necessary for the actual conditions to match the calibration conditions as long as all the orifices are maintained at the same temperature and upstream pressure. The actual flow through each orifice is calibrated under controlled conditions to give values that are used to determine the flow dilution ratios.[5] The flows from the orifices pass to three-way valves that can be set to direct the flow to either a vent or mixture outlet

where it is mixed with the by pass flow of the complementary component from a MFC. The total flow from the permeation vessel ( $Q_T$ ) is split between the critical orifices in the proportions shown in the schematic. The five three-way valves may be set in 32 combinations, thus enabling the flow at the output to be adjusted from zero to  $Q_T$  in steps of  $Q_T/31$ . Hence the volume fraction of the calibration component in the output can be varied in the ratio 1 to 31 with less than a 1% change in the output.

### 3.3 NATIONAL PHYSICAL LABORATORY, TEMPERATURE AND HUMIDITY GROUP (NPL-TH) METHOD

A schematic of the Low Frost-point Generator (LFG) [6] used by the Temperature and Humidity Group at NPL is given in figure 4. The NPL LFG is a primary standard of dew-point and frost-point temperature in the range from +20 °C to -90 °C (and experimentally down to -100 °C). Realisation of frost point is by saturation of air at selected controlled temperatures, and controlled pressure. The value of generated frost point is determined from measurements made using platinum resistance thermometers (PRTs). Traceability of measurement is provided by calibration of these thermometers to ITS-90 through NPL Temperature Standards. The uncertainty in the generated frost point is calculated by combining the estimated uncertainties arising from the calibration, drift, self heating and measurement of the PRTs, the saturation efficiency, temperature conditioning, pressure measurement and pressure differences in the calibration system, the temperature variations in the generator bath, and the effects of leaks, desorption and contamination. For reporting in the comparison, values of frost point were converted into values of amount fraction using vapour pressure formula due to Sonntag and water vapour enhancement factor due to Bögel [7].

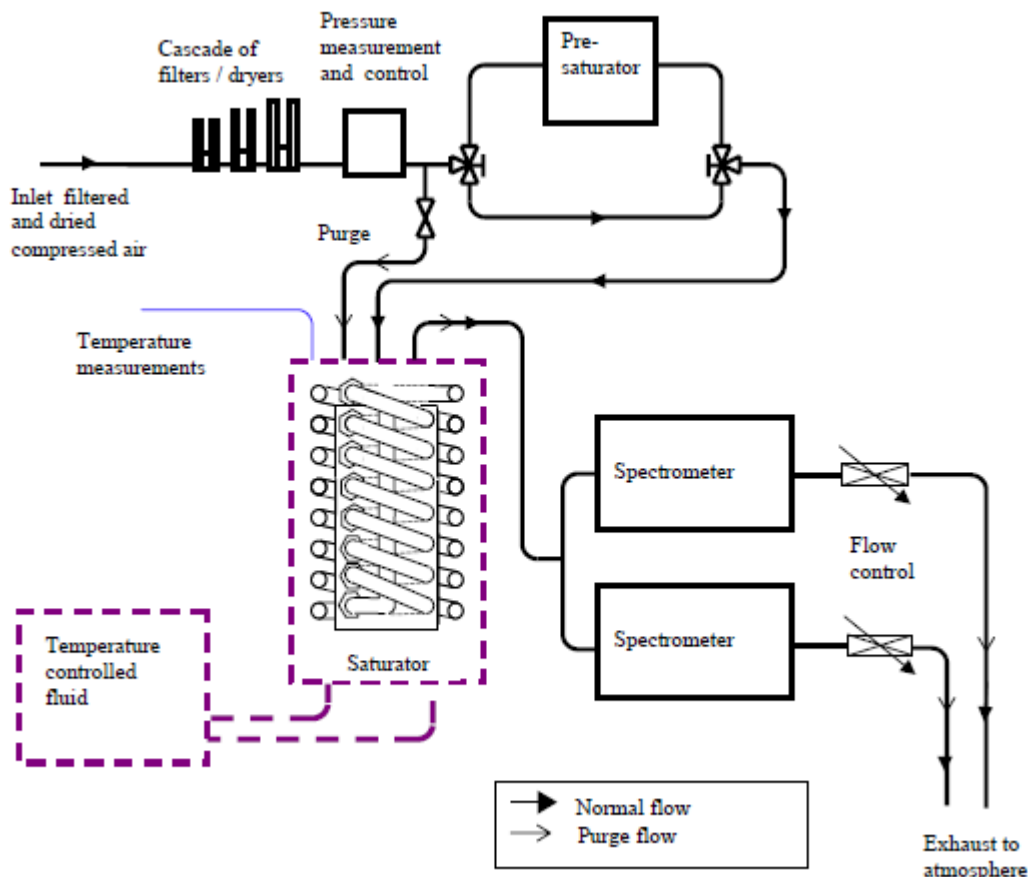


Figure 4 Schematic measurement layout of NPL Low Frost-Point Generator.

The sample air was supplied to the CRDS instrument inlets at the generator pressure of 115 kPa. The air outlet from each spectrometer was then vented to atmosphere, through a rotameter with a needle valve assembly for flow control. The outlet airflow was approximately 0.1 litres per minute. (This low flow rate was due to the limited inlet pressure, combined with the flow impedance of the spectrometers. Due to a misunderstanding, the spectrometers as supplied were not suitable for the relatively low inlet pressure supplied by the LFG.)

### 3.4 PHYSIKALISCH-TECHNISCHE BUNDESANSTALT (PTB) METHOD

Volume fractions of water vapour were generated by means of a Coulometric Trace Humidity Generator (CTHG). The CTHG operates on the principle of Faraday's law of electrolysis and is based on four processes:

- Generation of a zero gas stream of nitrogen containing a negligible amount of oxygen and water vapour.
- Generation of a defined quantity of hydrogen and oxygen by electrolysis of water in accordance with Faraday's law.
- Drying the partial gas flow from the electrolysis cell by a cold trap.
- Recombination of the generated hydrogen and oxygen back into water on a Pt/Pd-catalyst and addition of the generated water to the zero gas stream.

The volume fraction of water vapour is determined by the electrolytic current and the flow of the nitrogen carrier gas. The mixing ratio  $r$  of the moist gas produced by the CTHG is given by:

$$r = \frac{M_V}{M_{N_2}} \frac{V_0}{z F \dot{V}} \frac{I}{\dot{V}} \quad (6)$$

Where:  $I$  is the electrolysis current,  $\dot{V}$  is the flow of the reference gas at 0 °C and 1013.25 hPa,  $F$  is Faraday's constant,  $z$  is the number of the interchange charges (in this case  $z = 2$ ),  $M_V$  is the molecular weight of water,  $M_{N_2}$  is the molecular weight of nitrogen and  $V_0$  is the molar volume of the ideal gas.

If we consider the residual content of water vapour (blank) in the zero gas, we can calculate the volume fraction of water vapour:

$$\varphi = \frac{r}{\frac{M_V}{M_{N_2}} + r} + \text{blank} \quad (7)$$

A schematic of the CTHG is given in figure 5. The zero gas, taken from several cylinders of nitrogen, flows through two commercially available purification systems (adsorber and getter type). The residual oxygen and water vapour concentrations in the nitrogen are less than 1 nl/l volume fraction. At the inlet of the generator the zero gas stream is controlled by a needle valve and measured by a mass flow meter calibrated by the PTB laboratory of fluid mechanics. This flow meter returns the flow rate in standard litres per minute (flow rate at 0 °C, 1013,25 hPa), so that the mass of nitrogen can be calculated by means of the flow rate, the molecular weight of nitrogen and the molar volume of the ideal gas.

From the nitrogen main stream a small partial flow (ca. 5 l/h) is branched off to flush the electrolysis cell. This cell consists of a small glass cylinder with two platinum electrodes and diluted sulphuric acid solution as electrolyte. A known quantity of H<sub>2</sub> and O<sub>2</sub> is generated by electrolysis of water. The

$O_2$  and  $H_2$  produced and the undesirable vapour water resulting from the aqueous electrolysis solution, are transported by the nitrogen carrier gas through a cooling trap at a temperature of  $-160\text{ }^\circ\text{C}$ , where any water vapour delivered from the electrolysis cell is retained. This cooling trap, made from a stainless steel cylinder with a special internal structure, is a crucial point in the construction of the CTHG, because water vapour in the carrier gas is the largest contribution to the estimated uncertainty of reference mixtures generated at low amount fractions and determines the lower limit of the working range of the generator. The cooling temperature of  $-160\text{ }^\circ\text{C}$  is chosen to avoid condensation of oxygen. It is achieved by cooling with liquid nitrogen and using a low powered heating of the trap, suited to a lagging against direct contact of the cylinder with the liquid nitrogen.

After drying the gas stream from the electrolysis cell, the gas is driven through a Pd/Pt catalyst system at a temperature of  $190\text{ }^\circ\text{C}$ , where the desirable water vapour is obtained due to the catalytic process of recombination of  $H_2$  and  $O_2$  into  $H_2O$ . Then the humid nitrogen partial flow is added back to the nitrogen main stream, forming the reference gas.

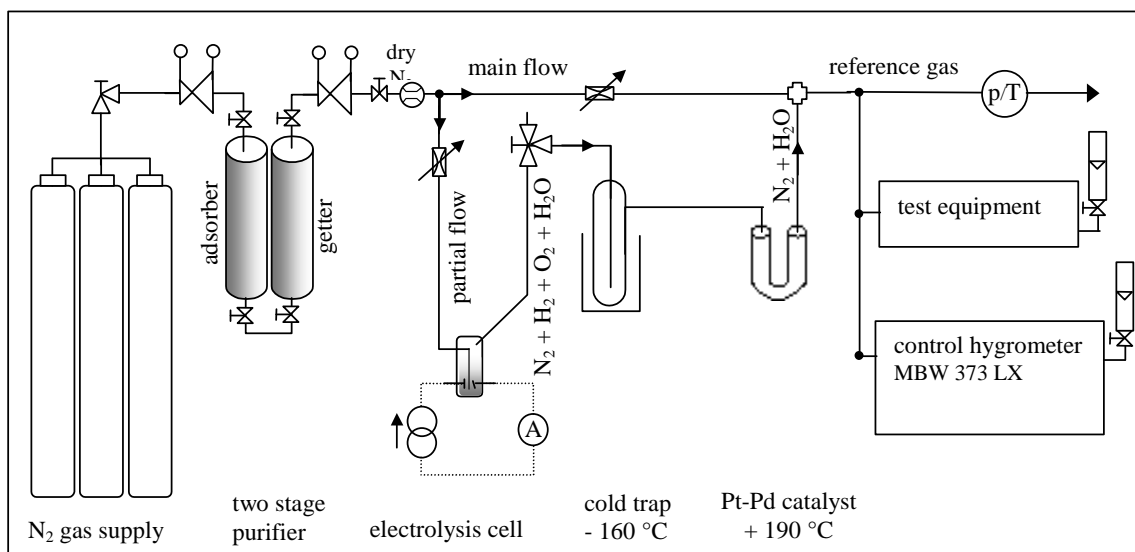


**Figure 5 Schematic of the Coulometric Trace Humidity Generator (CTHG) at PTB.**

The flow range of the reference gas covers 3 to 5 l/min. The gas pressure maintains an operating pressure between 1030 hPa and 1130 hPa to provide a sufficient flow through the test equipment. Pressure and temperature of the reference gas are measured in order to calculate the equivalent frost point temperature from the volume fraction of water vapour.

### 3.5 NATIONAL METROLOGY INSTITUTE OF JAPAN (NMIJ) METHOD

Trace water vapour in nitrogen gas was generated using a magnetic suspension balance/diffusion-tube humidity generator (MSB/DTG) developed at NMIJ.[8-10] The generation chamber of the DTG was attached to the bottom of the MSB with a common vacuum flange to form a closed system with the MSB. The MSB consisted of magnetic suspension coupling and an analytical balance. A diffusion cell (a small water container with a diffusion tube) in the generation chamber was magnetically suspended from the measuring load of the magnetic suspension coupling without contact with the analytical balance using the permanent magnet and the electromagnet. The pressure inside the chamber was controlled to 155 kPa using a pressure regulator. The temperature of the chamber was maintained at  $25\text{ }^\circ\text{C}$  or  $60\text{ }^\circ\text{C}$ . The water vapour from the diffusion cell was mixed with the dry nitrogen introduced from the inlet of the generation chamber. This humid gas was taken from the outlet of the generation chamber and further mixed with the dry nitrogen flowing from the bypass line. The evaporation rates of water vapour from the diffusion cell were measured as the mass-change rates of the diffusion cell using the MSB. The total flow rates of the dry nitrogen were accurately and precisely measured and controlled using a flow measurement /control system which uses a mass flow meter composed of

multiple critical flow Venturi nozzles (CFVNs), also known as sonic nozzles. The amount fractions of water vapour in nitrogen gas were calculated from the evaporation and flow rates.

Figure 6 shows a schematic of the facility.

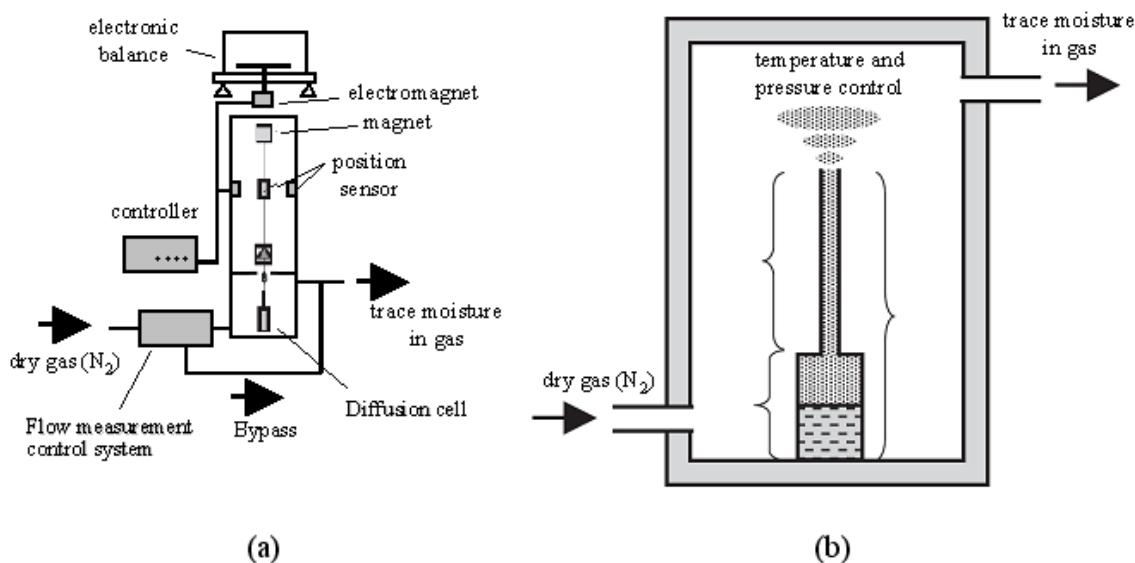


**Figure 6 Schematic of the NMIJ trace water vapour facility (a). The diffusion-tube trace-moisture generator is shown in (b).**

Travelling standards 1 and 2 were connected in series downstream of the MSB/DTG. Electropolished stainless steel tubes (SUS316L) were used. Before the measurement, a purge procedure was carried out for approximately three weeks using trace-moisture gas with an amount fraction of  $x_w=12$  nmol/mol generated by the DTG. The flow rate of the gas introduced in the spectrometers was estimated to be 0.5 l/min using a thermal mass flow meter.

#### 4 RESULTS

The stability and accuracy of travelling standard 1 were superior to travelling standard 2, so only data from travelling standard 1 are presented in the main body of this report. Measurements involving travelling standard 2 are presented in a separate annex at the end of this report.

All of the results using travelling standard 1 are presented in figure 7. Data from NPL-TH, whose matrix was air, exhibits a bias to the median of the results reported, ranging from 30 % at 10 nmol/mol to 10 % at 2000 nmol/mol (although the bias at and below 100 nmol/mol is less than the reported uncertainty of measurement). The data is also shown with an expanded scale in figure 8.

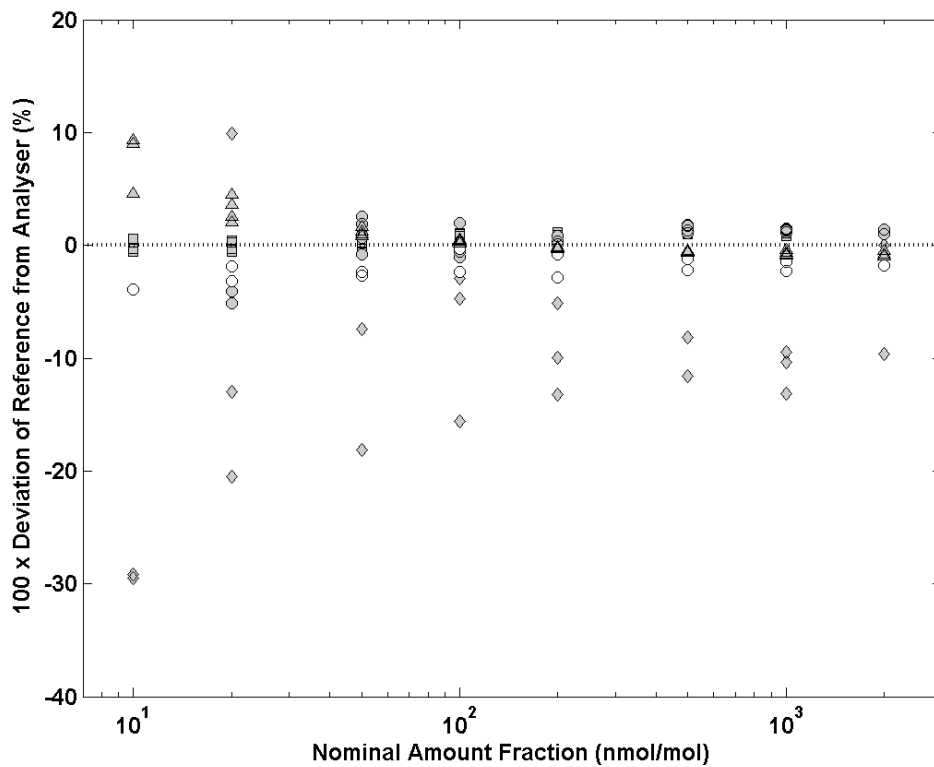


Figure 7 Deviation of the dynamic reference generated at each NMI from travelling standard 1. Data from NIST, NPL-GMTA, NPL-TH, PTB and NMIJ are represented with ○, ●, ◆, ▲ and ■ respectively.

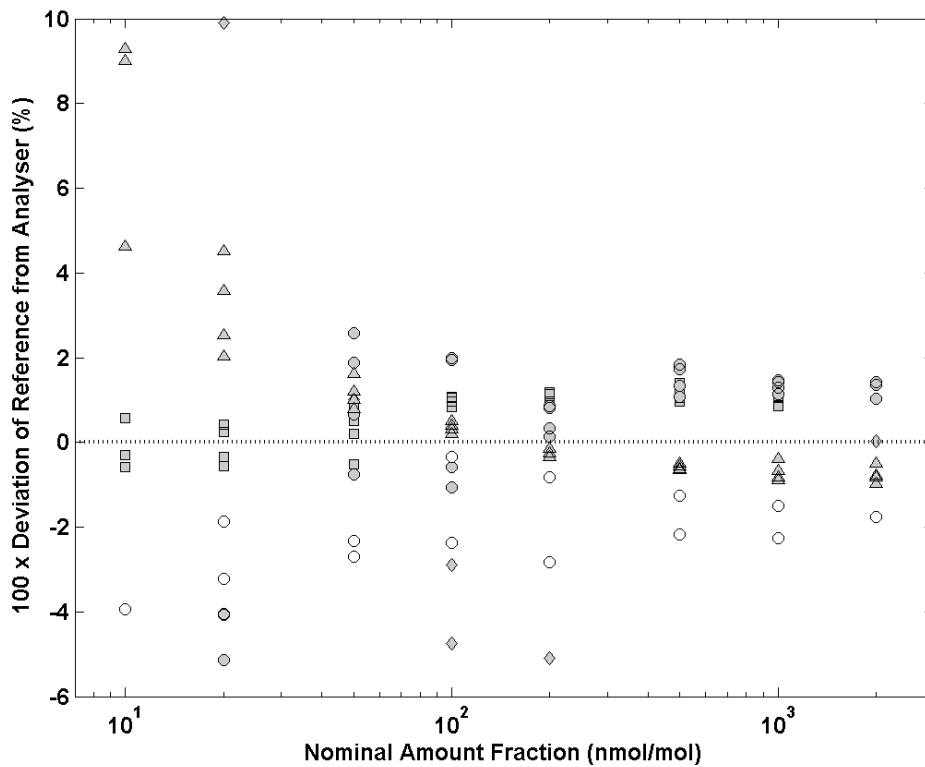


Figure 8 A reproduction of figure 7 with an expanded scale.



#### 4.1 CALCULATION OF REFERENCE VALUES

The reference values at each amount fraction were determined using a DerSimonian-Laird (DSL) algorithm [11] which has been recommended by the *ad hoc* Working Group on KCRV Calculation of the CCQM. The approach is based on the use of a weighted mean with an appropriate choice of weights.

DSL estimates an additional component of variance  $u^2(q)$  and combines this with the reported uncertainties  $u^2(x_i)$  to give the weights  $w_i$ , where  $x_i$  is the relative deviation of the dynamic reference from the travelling standard and  $q$  is a randomly varying quantity described by a probability distribution. The additional variance term is chosen so that the combination of reported variances and estimated additional variance is sufficient to account for the observed dispersion of values  $x_i$ .

$$x_{KCRV} = \sum_{i=1}^m w_i x_i \quad \text{and} \quad u(x_{KCRV}) = \left[ \frac{\sum_{i=1}^p w_i^2 (x_i - x_{KCRV})^2}{(1 - w_i)} \right]^{\frac{1}{2}} \quad (8)$$

where the weights are given by adding  $u(q)$  to the reported standard uncertainties  $u(x_i)$  in quadrature as follows

$$w_i = \frac{\frac{1}{u^2(x_i) + u^2(q)}}{\sum_{i=1}^m \frac{1}{u^2(x_i) + u^2(q)}} \quad (9)$$

The data from NPL-TH has not been used in the calculation of the reference values.

The degrees of equivalence  $d_i = x_i - x_{KCRV}$  have associated standard uncertainties

$$u^2(d_i) = u^2(x_i) + u^2(q) - u^2(x_{KCRV}) \quad (10)$$

if the value  $x_i$  is included in the calculation of the KCRV, and

$$u^2(d_i) = u^2(x_i) + u^2(q) + u^2(x_{KCRV}) \quad (11)$$

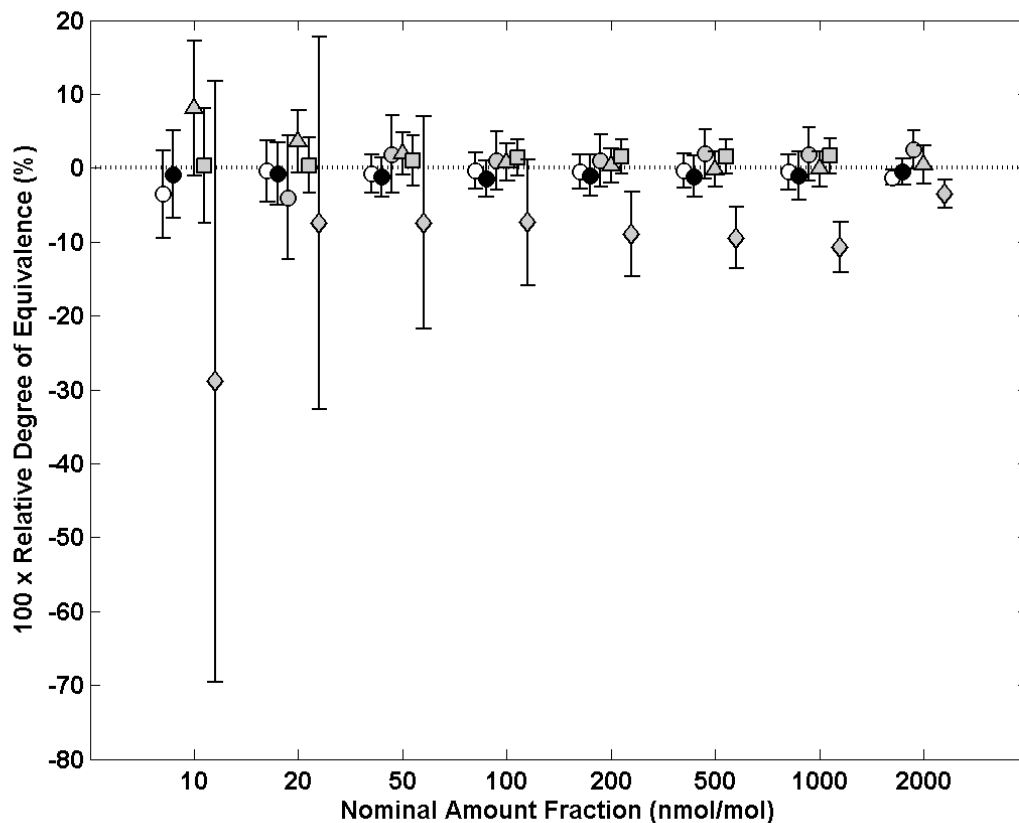
if the value  $x_i$  is not included in the calculation of the KCRV.

Table 3 gives the relative deviation of the dynamic reference from the travelling standard ( $x_i$ ), the degree of equivalence ( $d_i$ ) and the associated uncertainty ( $Ud_i$ ) for each NMI from travelling standard 1 at each amount fraction.

Table 3 Comparison results with travelling standard 1.

Nominal Amount Fraction (nmol/mol)	NIST 1			NPL-GMTA			NPL-TH		
	$x_i$	$d_i$	$U(d_i)$	$x_i$	$d_i$	$U(d_i)$	$x_i$	$d_i$	$U(d_i)$
10	-3.95	-3.51	5.92	-	-	-	-29.33	-28.90	40.63
20	-2.54	-2.11	4.21	-4.42	-3.99	8.42	-7.88	-7.45	25.23
50	-2.51	-1.73	2.63	1.09	1.87	5.28	-8.18	-7.40	14.41
100	-1.37	-0.97	2.44	0.57	0.97	3.97	-7.74	-7.35	8.52
200	-1.83	-1.32	2.31	0.53	1.04	3.52	-9.42	-8.91	5.73
500	-1.71	-1.29	2.33	1.49	1.91	3.37	-9.89	-9.47	4.17
1000	-1.88	-1.34	2.37	1.33	1.87	3.58	-11.29	-10.75	3.40
2000	-1.75	-0.49	0.98	1.28	2.54	2.60	-4.81	-3.55	1.92
Nominal Amount Fraction (nmol/mol)	PTB			NMIJ			NIST 2		
	$x_i$	$d_i$	$U(d_i)$	$x_i$	$d_i$	$U(d_i)$	$x_i$	$d_i$	$U(d_i)$
10	7.65	8.09	9.11	-0.11	0.33	7.78	-1.30	-0.86	5.92
20	3.17	3.60	4.21	-0.06	0.37	3.79	-1.17	-0.73	4.21
50	1.16	1.94	2.91	0.25	1.03	3.37	-2.02	-1.24	2.63
100	0.35	0.75	2.55	0.98	1.38	2.46	-1.91	-1.51	2.44
200	-0.22	0.28	2.34	1.03	1.54	2.32	-1.51	-1.00	2.31
500	-0.59	-0.17	2.34	1.15	1.57	2.33	-1.57	-1.15	2.33
1000	-0.70	-0.16	2.39	1.07	1.61	2.38	-1.60	-1.06	2.37
2000	-0.77	0.50	1.02	-	-	-	-1.78	-0.51	0.98

Figure 9 shows the relative degree of equivalence for each NMI from travelling standard 1 at each amount fraction. The data is also shown with an expanded scale in figure 10. Excellent comparability is demonstrated across the range of amount fractions measured. Data from NIST before (open circles) and after (black circles) the comparison provide an estimate of the drift of travelling standard 1. The difference between these measurements is negligible compared to the uncertainty reported by NIST, and to the deviation between participants. The upper limit on drift estimated from the two sets of measurements at NIST is much smaller than the “inter-laboratory uncertainty” term ( $u(q)$ ) estimated by the DSL method. Therefore we have assumed that the estimated values for  $u(q)$  are sufficient to allow for drift in the travelling standard.



**Figure 9** Relative degree of equivalence for each NMI using travelling standard 1 at each amount fraction. Data from NIST, NPL-GMTA, NPL-TH, PTB and NMIJ are represented with ○, ●, ◆, ▲ and ■ respectively. A second data set collected at NIST after the comparison is represented with ●. Bars indicate estimated uncertainties on the generated amount fractions of water by each institute at the 95% confidence interval.

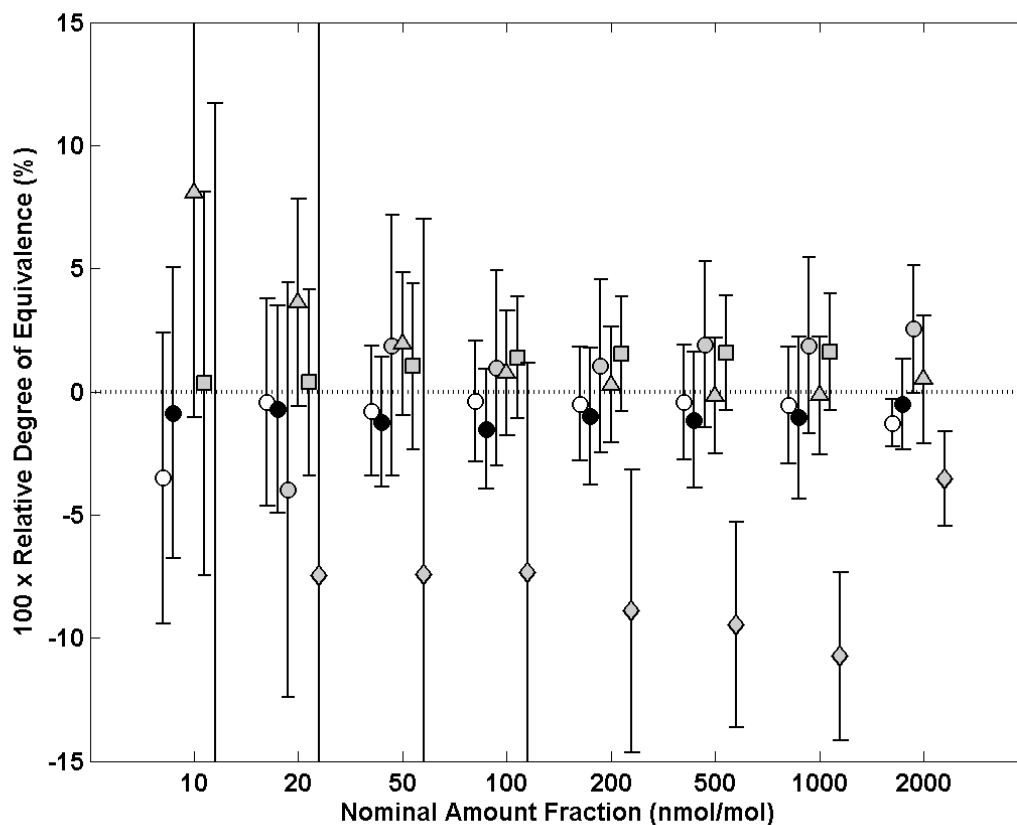


Figure 10 A reproduction of figure 9 with an expanded scale.

## 5 CONCLUSION

The results from the circulation of travelling standard 1 indicate comparability within the uncertainties for this comparison between NMIs using four entirely different methods to generate reference standards of water vapour in the range 10 to 2000 nmol/mol.

For the NPL-TH measurements in air, the high spectrometer readings may possibly be explained by unwanted absorption in oxygen. For this facility, therefore, the comparison results are inconclusive.

## 6 REFERENCES

- [1] A Wexler, *J. Res. National Bureau Standard*, **81A**, 5-19 (1977).
- [2] R W Hyland., A Wexler, *ASHRAE Transactions*, **89**, 520-535 (1983).
- [3] H Preston-Thomas, *Metrologia* **27**, 3-10, (1990).
- [4] G A Leggett, B A Goody, T D Gardiner, M J T Milton. Accurate, adjustable calibration source for measurements of trace water vapour, *Measurement and Control*, **40/9**, (2007).
- [5] P J Brewer, B A Goody, T Gillam, R J C Brown, M J T Milton, High accuracy stable gas flow dilution using a self- calibrating network of critical flow orifices, *Meas. Sci, Technol.*, **21**, 115902, (2010).
- [6] M Stevens, The New NPL Low Frost-point Generator, in Proceedings of *TEMPMEKO 99, 7<sup>th</sup> International Symposium on Temperature and Thermal Measurements in Industry and Science, Berlin, Germany, June 1999*, 321-326 (1999)
- [7] D Sonntag, Important new values of the physical constants of 1986, vapour pressure formulations based on the ITS-90, and psychrometer formulae. *Zeitschrift für Meteorologie*, 1990. **40(5)**, 340–344.
- [8] H Abe, H Tanaka, H Kitano, Uncertainty Analysis of Evaporation Rate in Magnetic Suspension Balance/Diffusion-Tube Humidity Generator, *Int J Thermophys*, 29:1555-1566, (2008).
- [9] H Abe, H Kitano, Improvement of flow and pressure controls in diffusion-tube humidity generator: Performance evaluation of trace moisture generation using cavity ring-down spectroscopy, *Sensor and Actuators A*, 165, 230-238, (2007).
- [10] H Abe, H Kitano, Development of humidity standard in trace-moisture region: Characteristics of humidity generation of diffusion tube humidity generator, *Sensor and Actuators A*, 128, 202-208, (2006).
- [11] R. DerSimonian and N. Laird, Meta-analysis in Clinical Trials, *Controlled Clinical Trials*, **7**, 177-188, (1986).

## 7 APPENDIX – DATA FROM PARTICIPANTS

**Table 4 Comparison results from NIST collected at the beginning of the comparison. The uncertainty in the reference values is provided at level of confidence of approximately 95% (k=2).**

date and approx time of measurement	nominal amount fraction (nmol/mol)	mean of NIST reference value (nmol/mol)	uncertainty of NIST reference value (nmol/mol)	travelling standard 1		travelling standard 2	
				amount fraction from analyser mean (nmol/mol)	1 standard dev. (nmol/mol)	amount fraction from analyser mean (nmol/mol)	1 standard dev. (nmol/mol)
18/10/2007 00:00	10	11.995	0.4	12.489	0.084	11.493	0.438
19/10/2007 00:00	20	20.021	0.4	20.686	0.156	19.886	0.651
22/10/2007 00:00	50	50.005	0.5	51.393	0.357	48.758	1.060
22/10/2007 00:00	100	100.215	0.7	102.659	0.840	97.078	1.663
23/10/2007 00:00	200	199.822	1.1	205.635	1.191	193.963	1.631
23/10/2007 00:00	500	500.223	2.4	511.287	3.099	476.969	2.147
24/10/2007 00:00	1000	1000.438	4.4	1023.650	4.183	968.987	2.716
26/10/2007 00:00	2000	2000.862	8.2	2036.602	6.155	2000.220	4.258
-	2000	-	8.2	-	-	-	-
29/10/2007 00:00	1000	1000.542	4.4	1015.661	2.646	995.193	3.257
31/10/2007 00:00	500	499.969	2.4	506.310	1.809	496.460	2.291
01/11/2007 00:00	200	200.001	1.1	201.663	1.102	198.398	1.731
02/11/2007 00:00	100	100.014	0.7	100.364	0.502	98.940	1.618
02/11/2007 00:00	50	50.021	0.5	51.211	0.207	50.711	1.496
05/11/2007 00:00	20	20.028	0.4	20.409	0.079	19.843	1.046
-	10	-	-	-	-	-	-
-	20	-	-	-	-	-	-
-	50	-	-	-	-	-	-
-	100	-	-	-	-	-	-
-	200	-	-	-	-	-	-
-	500	-	-	-	-	-	-
-	1000	-	-	-	-	-	-
-	2000	-	-	-	-	-	-
-	2000	-	-	-	-	-	-
-	1000	-	-	-	-	-	-
-	500	-	-	-	-	-	-
-	200	-	-	-	-	-	-
-	100	-	-	-	-	-	-
-	50	-	-	-	-	-	-
-	20	-	-	-	-	-	-
-	10	-	-	-	-	-	-

**Table 5 Comparison results from NPL-GMTA. The uncertainty in the gravimetric reference values is provided at level of confidence of approximately 95% (k=2).**

date and approx time of measurement	nominal amount fraction (nmol/mol)	mean of NPL gravimetric reference value (nmol/mol)	uncertainty of NPL gravimetric reference value (nmol/mol)	travelling standard 1		travelling standard 2	
				amount fraction from analyser mean (nmol/mol)	1 standard dev. (nmol/mol)	amount fraction from analyser mean (nmol/mol)	1 standard dev. (nmol/mol)
-	10	-	-	-	-	-	-
11/03/2008 13:00	20	22.3	1.9	23.3	0.5	25.9	0.4
11/03/2008 16:00	50	45.3	2.1	44.4	0.9	45.5	0.8
11/03/2008 19:00	100	92.5	3.0	90.7	1.4	89.5	1.0
12/03/2008 06:00	200	184.6	5.0	183.1	0.9	177.7	0.9
12/03/2008 09:00	500	505.0	12.5	498.4	3.1	476.1	1.2
12/03/2008 13:00	1000	1050.4	28.5	1035.2	6.5	973.2	4.4
12/03/2008 16:00	2000	2074.8	50.6	2053.5	9.6	1925.0	8.8
12/03/2008 19:00	2000	2074.9	50.6	2047.0	7.0	1954.1	6.8
13/03/2008 06:00	1000	1048.1	28.4	1036.4	4.5	993.2	4.2
13/03/2008 10:00	500	504.6	12.5	496.0	3.9	489.3	1.6
13/03/2008 13:00	200	184.5	5.0	184.2	0.9	185.3	0.8
13/03/2008 15:00	100	92.4	3.0	93.4	1.0	96.8	0.8
17/03/2008 13:00	50	45.3	2.1	45.0	0.9	46.3	0.8
17/03/2008 16:00	20	22.4	1.9	23.3	0.6	25.1	0.4
-	10	-	-	-	-	-	-
-	20	-	-	-	-	-	-
18/03/2008 07:00	50	45.3	2.1	44.2	0.8	44.5	0.7
18/03/2008 10:00	100	92.6	3.0	90.8	1.5	87.8	1.3
18/03/2008 13:00	200	184.7	5.0	183.1	1.6	174.0	1.1
18/03/2008 16:00	500	505.1	12.5	496.0	1.7	474.3	1.4
19/03/2008 06:00	1000	1051.0	28.5	1037.7	4.8	988.3	3.9
19/03/2008 12:00	2000	2075.3	50.6	2046.0	9.8	1955.7	5.7
-	2000	-	-	-	-	-	-
19/03/2008 15:00	1000	1050.8	28.5	1036.1	7.0	1005.3	6.9
20/03/2008 06:00	500	504.9	12.5	499.5	1.3	481.8	1.7
20/03/2008 09:00	200	184.5	5.0	183.9	1.5	183.2	1.3
20/03/2008 11:00	100	92.6	3.0	93.1	1.5	95.1	1.1
20/03/2008 14:00	50	45.3	2.1	45.6	1.1	48.9	0.8
20/03/2008 16:00	20	22.3	1.9	23.6	0.6	26.9	0.4
-	10	-	-	-	-	-	-

**Table 6 Comparison results from NPL-TH. The uncertainty in the reference values is provided at level of confidence of approximately 95% (k=2).**

date and approx time of measurement	nominal amount fraction (nmol/mol)	mean of NPL reference value (nmol/mol)	uncertainty of NPL reference value (nmol/mol)	travelling standard 1		travelling standard 2	
				amount fraction from analyser		amount fraction from analyser	
				mean (nmol/mol)	1 standard dev. (nmol/mol)	mean (nmol/mol)	1 standard dev. (nmol/mol)
-	10	12.127	4	17.12	2.5	18.02	2.5
-	20	19.194	5	17.46	5.5	19.65	5.5
-	50	64.748	7	64.10	7.0	67.86	7.0
-	100	96.073	8	98.94	7.0	98.36	7.0
-	200	149.110	10	157.13	8.0	155.43	8.0
-	500	419.688	15	457.06	11.0	439.14	11.0
-	1000	998.815	17	1103.09	12.5	1039.25	12.5
-	2000	2112.385	27	2337.94	14.5	2242.02	14.5
-	2000	-	-	-	-	-	-
-	1000	937.319	17	1078.89	12.5	1012.63	12.5
-	500	491.858	15	556.42	11.0	531.39	11.0
-	200	191.960	10	221.16	8.0	215.12	8.0
-	100	91.080	8	107.91	7.0	109.17	7.0
-	50	47.340	7	57.81	7.0	60.49	7.0
-	20	36.519	5	45.96	5.5	49.55	5.5
-	10	13.895	4	19.71	2.5	21.63	2.5
-	20	36.121	5	41.52	5.5	43.09	5.5
-	50	70.337	7	75.99	7.0	75.13	7.0
-	100	85.386	8	89.63	7.0	90.55	7.0
-	200	218.590	10	242.74	8.0	232.29	8.0
-	500	-	-	-	-	-	-
-	1000	872.509	17	973.69	12.5	924.46	12.5
-	2000	2049.144	27	2048.75	14.5	2190.74	14.5
-	2000	-	-	-	-	-	-
-	1000	-	-	-	-	-	-
-	500	-	-	-	-	-	-
-	200	-	-	-	-	-	-
-	100	-	-	-	-	-	-
-	50	-	-	-	-	-	-
-	20	-	-	-	-	-	-
-	10	-	-	-	-	-	-



**Table 7 Comparison results from PTB. The uncertainty in the reference values is provided at level of confidence of approximately 95% (k=2). Measurements on travelling standards 1 and 2 were not performed simultaneously. Hence the first and second values in the gravimetric reference column refer to mixtures supplied to travelling standards 1 and 2 respectively.**

date and approx time of measurement	nominal amount fraction (nmol/mol)	mean of PTB reference value (nmol/mol)	uncertainty of PTB reference value (nmol/mol)	travelling standard 1		travelling standard 2	
				amount fraction from analyser	amount fraction from analyser	amount fraction from analyser	amount fraction from analyser
				mean (nmol/mol)	1 standard dev. (nmol/mol)	mean (nmol/mol)	1 standard dev. (nmol/mol)
-	10	10.11	0.80	9.25	0.25	-	-
-	20	20.8 / 20.8	0.80	19.9	0.10	20.3	0.25
-	50	50.1 / 50.7	0.80	49.6	0.25	49.2	0.25
-	100	100.1 / 100.1	1.00	99.8	0.40	96.0	0.40
-	200	201.5 / 200.0	1.30	202.0	0.75	193.4	0.75
-	500	499.2 / 498.5	2.60	502.0	2.50	486.1	1.50
-	1000	993.0 / 993.0	5.30	1002.0	3.50	965.5	3.50
-	2000	1999.5 / 2004.0	10.00	2015.0	10.00	1958.0	5.00
-	2000	1999.9 / 2014.0	10.00	2010.0	10.00	1966.0	5.00
-	1000	1006.0 / 1006.0	5.30	1010.0	3.50	984.5	3.50
-	500	501.0 / 503.2	2.60	503.5	2.50	489.0	1.50
-	200	200.0 / 200.1	1.30	200.3	0.75	192.9	0.75
-	100	100.7 / 101.0	1.00	100.5	0.40	98.4	0.40
-	50	50.5 / 50.5	0.80	50.1	0.25	49.7	0.25
-	20	20.2 / 20.2	0.80	19.5	0.10	19.3	0.25
-	10	11.12	0.80	10.20	0.25	-	-
-	20	20.2 / 20.4	0.80	19.7	0.10	19.2	0.25
-	50	50.3 / 50.3	0.80	49.5	0.25	48.3	0.25
-	100	100.0 / 100.2	1.00	99.6	0.40	98.2	0.40
-	200	199.9 / 200.2	1.30	200.6	0.75	194.3	0.75
-	500	500.7 / 500.2	2.60	504.0	2.50	486.3	1.50
-	1000	1000.8 / 1000.8	5.30	1007.5	3.50	976.3	3.50
-	2000	1988.6 / 2002.9	10.00	2005.0	10.00	1952.0	5.00
-	2000	1995.3 / 2002.5	10.00	2015.0	10.00	1950.0	5.00
-	1000	1001.6 / 1005.4	5.30	1010.0	3.50	976.1	3.50
-	500	500.8 / 500.8	2.60	504.0	2.50	485.2	1.50
-	200	200.2 / 201.6	1.30	200.5	0.75	197.4	0.75
-	100	100.1 / 101.0	1.00	99.6	0.40	96.6	0.40
-	50	50.4 / 50.0	0.80	49.8	0.25	47.4	0.25
-	20	20.1 / 20.4	0.80	19.7	0.10	20.0	0.25
-	10	10.62	0.80	10.2	0.25	-	-

**Table 8 Comparison results from NMIJ. The uncertainty in the gravimetric reference values is provided at level of confidence of approximately 95% (k=2).**

date and approx time of measurement	nominal amount fraction (nmol/mol)	mean of NMIJ gravimetric reference value (nmol/mol)	uncertainty of NMIJ gravimetric reference value (nmol/mol)	travelling standard 1		travelling standard 2	
				amount fraction from analyser		amount fraction from analyser	
				mean (nmol/mol)	1 standard dev. (nmol/mol)	mean (nmol/mol)	1 standard dev. (nmol/mol)
02/04/2009 14:40	10	12.48	0.67	12.522	0.052	12.61	0.64
03/04/2009 05:40	20	20.39	0.77	20.508	0.069	20.13	0.61
03/04/2009 20:40	50	50.91	1.36	51.18	0.22	49.06	0.35
07/04/2009 18:30	100	100.54	0.79	99.58	0.51	96.36	0.49
08/04/2009 04:30	200	222.45	1.27	219.97	0.68	210.07	0.62
08/04/2009 14:30	500	518.3	2.68	511.2	1.4	487.6	1.4
09/04/2009 00:30	1000	1006.4	5.10	995.9	3.8	952.7	2.6
-	2000	-	-	-	-	-	-
-	2000	-	-	-	-	-	-
09/04/2009 18:10	1000	1003.2	4.64	992.2	4.0	951.9	2.4
10/04/2009 09:10	500	517.5	2.45	512.5	1.7	493.1	1.1
11/04/2009 00:10	200	222.23	1.18	219.62	0.75	213.74	0.52
11/04/2009 15:10	100	100.34	0.76	99.27	0.53	97.73	0.49
12/04/2009 19:40	50	52.17	1.05	51.74	0.15	51.39	0.32
13/04/2009 20:40	20	20.90	0.69	20.85	0.09	21.95	0.64
14/04/2009 21:40	10	12.80	0.64	12.726	0.067	14.03	0.19
15/04/2009 23:00	20	20.78	0.76	20.69	0.11	20.84	0.11
16/04/2009 14:00	50	51.88	1.32	51.62	0.26	50.51	0.34
17/04/2009 18:10	100	99.54	0.79	98.50	0.56	94.49	0.45
18/04/2009 04:10	200	220.53	1.29	218.50	0.38	208.13	0.74
18/04/2009 14:10	500	513.2	2.72	507.9	1.0	483.6	1.4
19/04/2009 00:10	1000	995.2	5.17	982.8	4.4	942.8	2.4
-	2000	-	-	-	-	-	-
-	2000	-	-	-	-	-	-
21/04/2009 09:50	1000	994.4	4.17	985.9	3.2	945.5	2.9
22/04/2009 00:50	500	512.5	2.21	506.4	3.1	487.4	1.5
22/04/2009 15:50	200	220.32	1.10	218.39	0.77	211.43	0.77
23/04/2009 06:50	100	99.46	0.73	98.63	0.51	95.92	0.39
24/04/2009 17:00	50	51.34	0.95	51.24	0.19	50.31	0.23
25/04/2009 18:00	20	20.58	0.67	20.65	0.13	20.87	0.20
26/04/2009 09:00	10	12.61	0.63	12.681	0.055	13.67	0.37



8 ANNEX

Figure 11 shows the results using travelling standard 2. A similar bias to the data from travelling standard 1 is observed from NPL-TH. As before, the data is also shown with an expanded scale in figure 12.

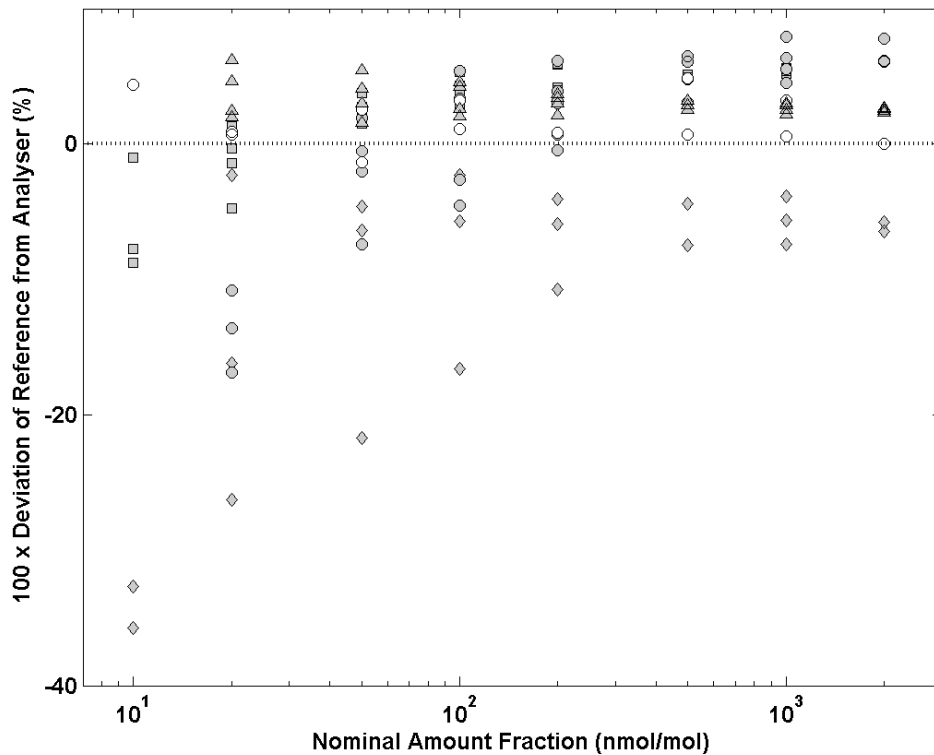


Figure 11 Deviation of the dynamic reference generated at each NMI from travelling standard 2. Data from NIST, NPL-GMTA, NPL-TH, PTB and NMIJ are represented with ○, ●, ◆, ▲ and ■ respectively.

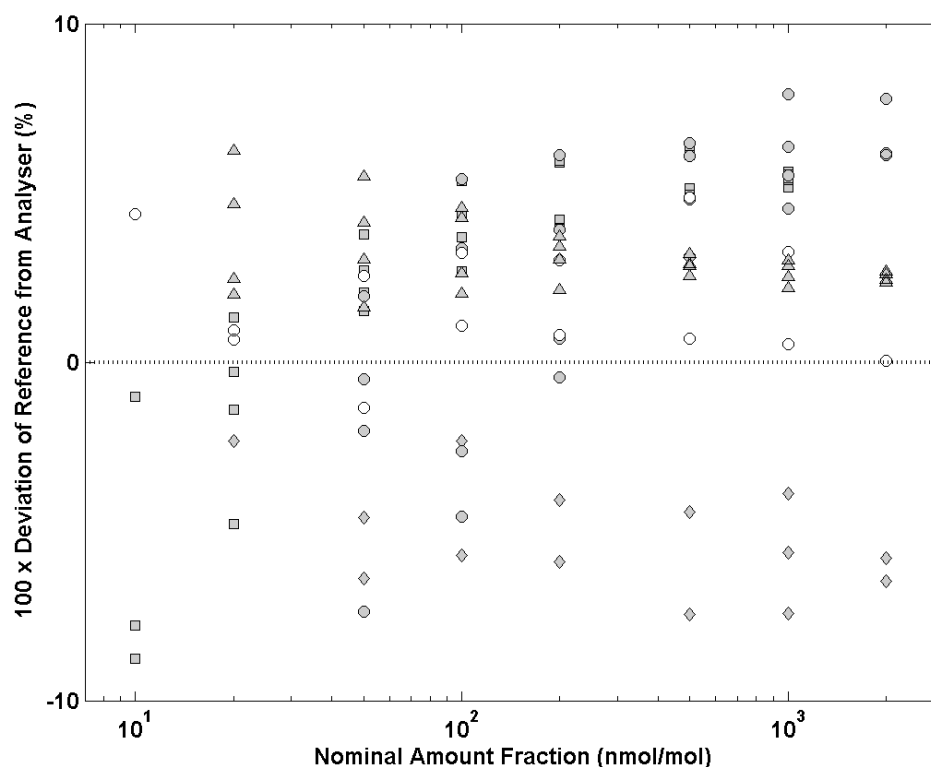


Figure 12 A reproduction of figure 11 with an expanded scale.

Table 10 gives the relative deviation of the dynamic reference from the travelling standard ( $x_i$ ), the degree of equivalence ( $d_i$ ) and the associated uncertainty ( $U(d_i)$ ) for each NMI from travelling standard 2 at each amount fraction.

Table 10 Comparison results with travelling standard 2.

Nominal Amount Fraction (nmol/mol)	NIST 1			NPL-GMTA			NPL-TH		
	$x_i$	$d_i$	$U(d_i)$	$x_i$	$d_i$	$U(d_i)$	$x_i$	$d_i$	$U(d_i)$
10	4.37	-7.50	36.94		-	-	-34.23	-46.11	65.40
20	0.80	1.71	7.13	-13.77	-12.86	10.20	-14.93	-14.02	26.37
50	0.60	-0.68	2.42	-1.99	-3.27	5.18	-10.90	-12.18	14.35
100	2.16	-0.01	3.10	0.39	-1.78	4.41	-8.20	-10.37	8.83
200	1.91	-1.29	2.77	2.57	-0.63	3.84	-6.91	-10.12	6.06
500	2.79	-1.21	2.77	5.12	1.12	3.69	-5.93	-9.94	4.61
1000	1.89	-1.94	3.28	6.08	2.25	4.23	-5.66	-9.49	4.63
2000	0.03	-2.70	1.83	6.69	3.96	3.02	-6.12	-8.85	5.46
Nominal Amount Fraction (nmol/mol)	PTB			NMIJ			NIST 2		
	$x_i$	$d_i$	$U(d_i)$	$x_i$	$d_i$	$U(d_i)$	$x_i$	$d_i$	$U(d_i)$
10		-	-	-5.85	-17.73	37.28	36.88	25.01	36.94
20	3.84	4.75	7.13	-1.29	-0.38	6.89	0.26	1.17	7.13
50	3.57	2.29	2.72	2.51	1.23	3.21	0.17	-1.12	2.42
100	3.38	1.21	3.18	4.01	1.84	3.11	0.17	-2.00	3.10
200	3.08	-0.13	2.80	5.01	1.80	2.79	-	-	-
500	2.88	-1.12	2.78	5.62	1.62	2.77	-	-	-
1000	2.64	-1.19	3.29	5.44	1.61	3.29	-	-	-
2000	2.52	-0.21	1.86	-	-	-	-	-	-

Figure 13 shows the relative degree of equivalence for each NMI from travelling standard 2 at each amount fraction. The reference values at each amount fraction were determined by using the same methodology employed for figures 9 and 10. The data is also shown with an expanded scale in figure 14. Excellent comparability is demonstrated across the range of amount fractions measured (with the exception of 10 nmol/mol). A bias is evident at amount fractions above 100 nmol/mol. Data from NIST before (open circles) and after (black circles) the comparison provide an indication of the drift of travelling standard 2 at four different amount fractions. The difference between these measurements above 10 nmol/mol is negligible compared to the deviation between participants.

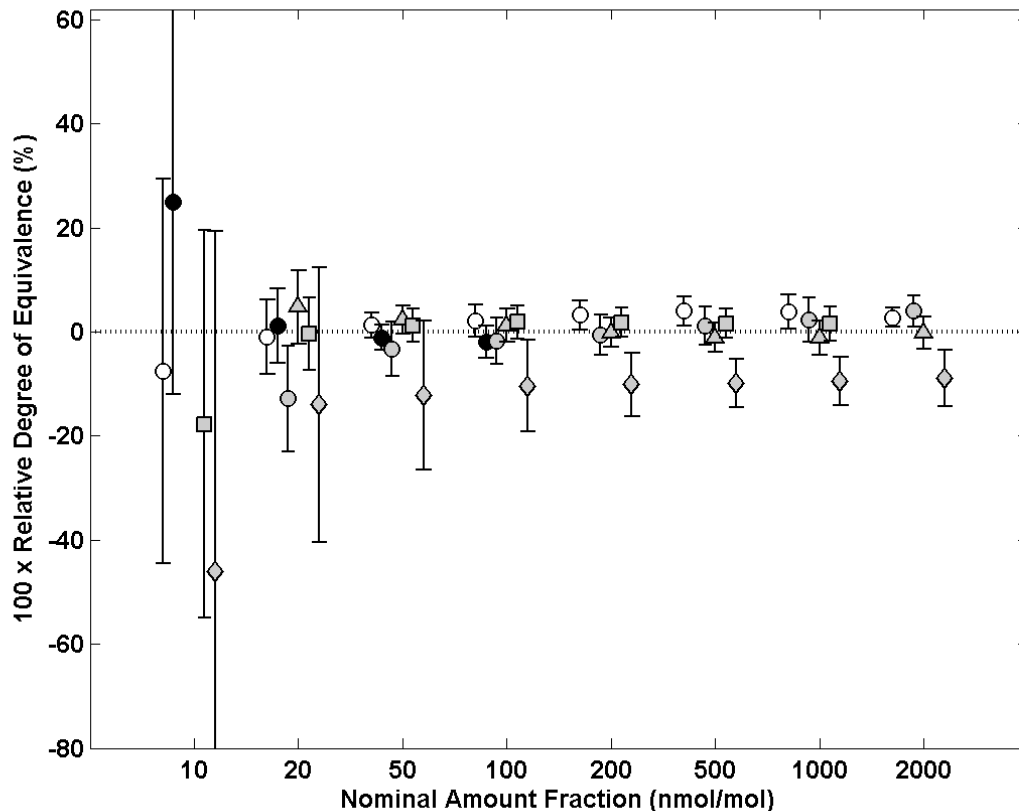


Figure 13 Relative degree of equivalence for each NMI using travelling standard 2 at each amount fraction. Data from NIST, NPL-GMTA, NPL-TH, PTB and NMII are represented with ○, ●, ◆, ▲ and ■ respectively. A second data set collected at NIST after the comparison is represented with ●. Bars indicate estimated uncertainties on the generated amount fractions of water by each institute at the 95% confidence interval.

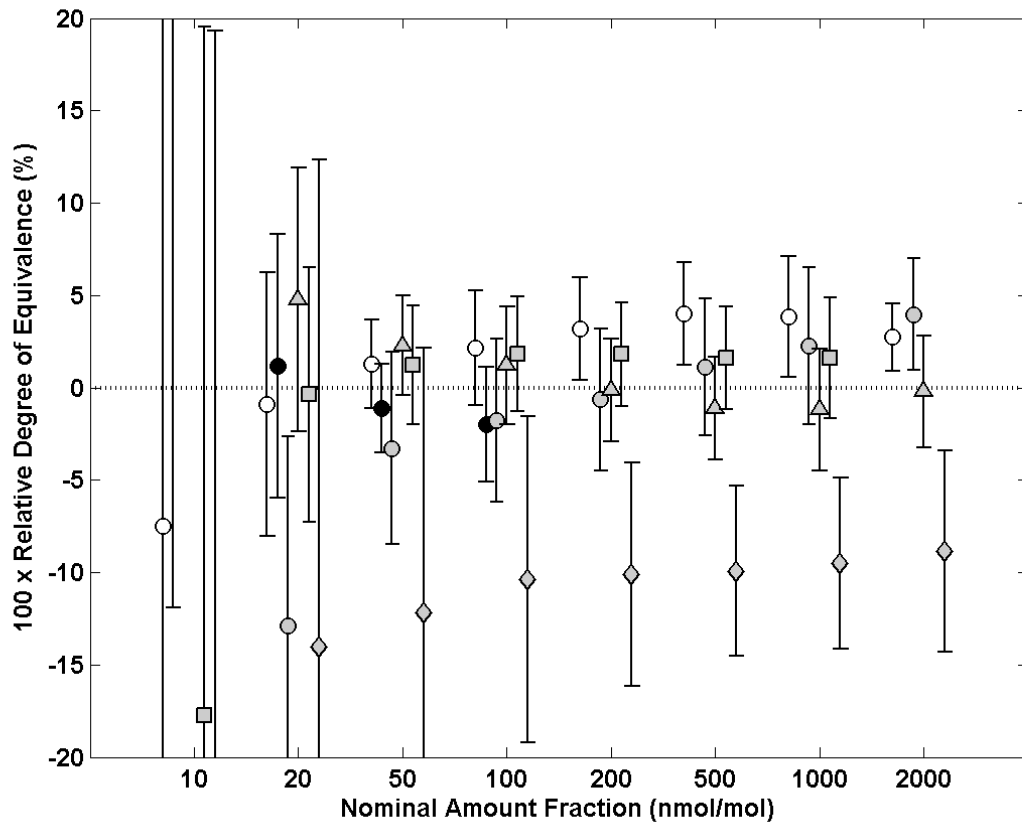


Figure 14 A reproduction of figure 13 with an expanded scale.